A fourth-order algorithm for solving the multi-dimensional Kramers equation in Langevin form

2009 J. Phys. A: Math. Theor. 42 315002

(http://iopscience.iop.org/1751-8121/42/31/315002)

IOP PUBLISHING JOURNAL OF PHYSICS A: MATHEMATICAL AND THEORETICAL

J. Phys. A: Math. Theor. **42** (2009) 315002 (14pp) doi:10.1088/1751-8113/42/31/315002

A fourth-order algorithm for solving the multi-dimensional Kramers equation in Langevin form

I Vadeiko[1] **and F Drolet**[1,2]

[1] FPInnovations, 570 boul. St-Jean, Pointe-Claire, Québec H9R 3J9, Canada
[2] Physics Department, McGill University, 3600 rue Université, Montreal, Québec H3A 2T8, Canada

E-mail: Ilya.Vadeiko@fpinnovations.ca and Francois.Drolet@fpinnovations.ca

Received 20 April 2009, in final form 10 June 2009
Published 15 July 2009
Online at stacks.iop.org/JPhysA/42/315002

Abstract

We propose a new fourth-order numerical method for solving the multi-dimensional Kramers equation in standard and overdamped regimes. The algorithm is developed for modelling the trajectories of airborne particles propagating through porous media such as three-dimensional fibre networks. It disentangles the deterministic and stochastic parts of the solution, so that standard fourth-order numerical methods can be used to calculate the deterministic component. The stochastic correction to the solution is obtained using a perturbative expansion of the stochastic force. In the overdamped regime, our method avoids the need for extremely small time steps required by conventional methods. We compare the convergence rate of our algorithm to that of other methods by solving the one-dimensional Duffing equation. The proposed algorithm is finally used to evaluate the performance of various filters made from fibres of two different sizes.

PACS numbers: 2.70, 05.40, 02.50

1. Introduction

A great number of physical problems involving interactions between a deterministic system and a large, statistically described environment require solving stochastic differential equations (SDEs). Effective and stable algorithms for solving such equations numerically are always in demand and various second- and fourth-order numerical methods have been proposed [1–10]. The particular problem considered here is the motion of airborne particles through fibrous filters. Specifically, we need to construct the trajectories of a large number of airborne particles of varying sizes and evaluate how the probability of capture of these particles changes with the composition of the filter. We assume that the particles are spherical and non-interacting, and we neglect any disturbance of the air flow field they may cause. Furthermore,

for the particle sizes of interest (a few microns at most), the gravitational force is negligible compared to the drag force exerted by the air flow. As a result, the only relevant forces acting on the particles are the drag force and Brownian diffusion in the air flow. The motion of each particle is then governed by a special type of SDEs called the Kramers equation [11]:

$$\dot{\vec{x}} = \vec{v}, \tag{1}$$

$$\dot{\vec{v}} = \gamma(\vec{V} - \vec{v}) + \vec{\Gamma}. \tag{2}$$

These equations apply to many other phenomena such as stochastically driven oscillators [12–15] and rectified Brownian motion in molecular and cell biology [16, 17]. In our case, $\vec{x}$ and $\vec{v}$ denote the position and velocity of the particle's centre of mass and $\vec{V}(\vec{x})$ is the stationary air velocity at point $\vec{x}$. $\vec{V}$ represents the drag force normalized to velocity units. $\vec{\Gamma}$ is a Langevin force and γ is a relaxation rate given by the expression $\gamma = 3\pi d_p \mu / m C_c$, where m and d_p are the mass and diameter of the particle and μ is the viscosity of air. Cunninghman's slip correction to Stokes law is $C_c = 1 + K_n\left(1.142 + 0.558\, \mathrm{e}^{-\frac{0.999}{K_n}}\right)$, where $K_n = 2\lambda/d_p$ is the Knudsen number and $\lambda = 6.64 \times 10^{-8}$ m is the mean free path of air molecules. The Langevin force $\vec{\Gamma}$ in equation (2) is a zero-mean Gaussian noise. Its correlation function reads

$$\langle \Gamma_i(t)\Gamma_j(t')\rangle = q\delta_{ij}\delta(t - t'), \tag{3}$$

where q is the noise strength, which depends on the physical parameters of the particular problem under consideration. In our case, $q = \frac{2kT}{m}\gamma$, where kT defines the thermal energy. The parameter γ thus determines the intensity of both the drag force and the noise term. It increases nonlinearly with decreasing particle diameter and can run across a large range of values. As γ becomes large, existing explicit algorithms discussed below quickly become inefficient as they require a time step Δt such that the product $\gamma \Delta t$ remains below 1.

In this paper, we propose a unified multi-dimensional approach for solving the Kramers equation for a wide range of γ values. In our algorithm, we disentangle the deterministic and stochastic parts of the solution which allows us to use existing fourth-order numerical methods for calculating the deterministic part. In the limit of large γ, we are therefore able to use existing implicit schemes with adaptive step size control to find the deterministic component of the solution at a given Δt without reducing the time step to extremely small values. At each iteration, we then calculate the stochastic correction to the deterministic component. By focusing on the slowly varying component of the solution, we are able to overcome the limitation $\gamma \Delta t < 1$ and to achieve a significant improvement in convergence at relatively large values of $\gamma \Delta t$. For the problem of airborne particle diffusion, the method allows us to efficiently construct the trajectories of particles ranging in size from several nanometres to several microns.

The remainder of this paper is organized as follows. In the following section, we construct two forms of the algorithm appropriate for the regular and overdamped regimes, respectively. In section 3, we consider the one-dimensional Duffing equation and compare the convergence of our algorithm to other methods. We then apply the algorithm to the study of airborne particles propagating through a fibrous network (section 4). Specifically, we evaluate the efficiency of model filters created by mixing fibres of two different sizes in different proportions and compare our results to published data. Concluding remarks are provided in section 5.

2. Derivation of the algorithms

The formal solution to equations (1) and (2) is given by

$$\vec{x}(t + \Delta t) = \vec{x}(t) + \int_0^{\Delta t} \vec{v}(t + t')\, \mathrm{d}t', \tag{4}$$

$$\vec{v}(t+\Delta t) = \vec{v}(t)\,\mathrm{e}^{-\gamma\Delta t} + \gamma\int_0^{\Delta t}\mathrm{e}^{-\gamma(\Delta t-t')}\vec{V}(\vec{x}(t+t'))\,\mathrm{d}t' + \int_0^{\Delta t}\mathrm{e}^{-\gamma(\Delta t-t')}\vec{\Gamma}(t+t')\,\mathrm{d}t'. \quad (5)$$

Both expressions have a nontrivial dependence on the stochastic component through the drag force term $\vec{V}\left(\vec{x}(t')\right)$. The influence of the Langevin force can be represented as a correction to the solution of the deterministic equation, i.e.

$$\Delta\vec{x}(\Delta t) \equiv \vec{x}(t+\Delta t) - \vec{x}(t) = \Delta\vec{x}^{\,D} + \Delta\vec{x}^{\,S}. \quad (6)$$

In the above equation, the superscript D denotes the deterministic solution obtained by solving equation (2) in the absence of the last term, and S denotes the stochastic correction due to the Langevin force. A similar expression holds for $\Delta\vec{v}$.

Assuming that the drag force $\vec{V}\,(\vec{x})$ is a smooth function of the coordinates, we can expand it in a Taylor series with respect to the stochastic correction:

$$V_i(\vec{x}(t+\Delta t)) = V_i(\vec{x}(t)+\Delta\vec{x}^{\,D}) + V_i^{(\alpha)}\Delta x_\alpha^S + \tfrac{1}{2}V_i^{(\alpha,\beta)}\Delta x_\alpha^S\Delta x_\beta^S + \cdots. \quad (7)$$

Here, the superscripts α and β denote partial derivatives, while subscripts are used to identify vector components. The rule of summation over repeated indices is assumed. Furthermore, since all force derivatives are taken at point $\vec{x}(t)+\Delta\vec{x}^{\,D}$, the solution can be decomposed into a deterministic and a stochastic part. Substituting equation (7) into the solution for the velocity equation (5) yields the following expressions for the velocity increments:

$$\begin{aligned}\Delta v_i^D &= v_i(t)(\mathrm{e}^{-\gamma\Delta t}-1) + \gamma\int_0^{\Delta t}\mathrm{e}^{-\gamma(\Delta t-t')}V_i(\vec{x}(t)+\Delta\vec{x}^{\,D}(t'))\,\mathrm{d}t',\\ \Delta v_i^S &= W_i(\Delta t,\gamma) + \gamma\int_0^{\Delta t}\mathrm{e}^{-\gamma(\Delta t-t')}\left[V_i^{(\alpha)}\Delta x_\alpha^S(t') + \frac{1}{2}V_i^{(\alpha,\beta)}\Delta x_\alpha^S(t')\Delta x_\beta^S(t') + \cdots\right]\mathrm{d}t'. \quad (8)\end{aligned}$$

Substituting equations (8) into equation (4) we then obtain a general integral equation for the stochastic increments of the coordinates:

$$\begin{aligned}\Delta x_i^S(\Delta t) = W_i^{[1]}(\Delta t,\gamma) + \gamma\int_0^{\Delta t}\mathrm{d}t'\int_0^{t'}\mathrm{e}^{-\gamma(t'-t'')}\\ \times\left[V_i^{(\alpha)}\Delta x_\alpha^S(t'') + \frac{1}{2}V_i^{(\alpha,\beta)}\Delta x_\alpha^S(t'')\Delta x_\beta^S(t'') + \cdots\right]\mathrm{d}t''. \quad (9)\end{aligned}$$

In the above equations, we introduced the functions

$$\overrightarrow{W}(\Delta t,\omega) = \int_0^{\Delta t}\mathrm{e}^{-\omega(\Delta t-t')}\vec{\Gamma}(t+t')\,\mathrm{d}t', \quad (10)$$

$$\overrightarrow{W}^{[1]}(\Delta t,\omega) = \int_0^{\Delta t}\overrightarrow{W}(t',\omega)\,\mathrm{d}t' = -\frac{\overrightarrow{W}(\Delta t,\omega)-\overrightarrow{W}(\Delta t,0)}{\omega}, \quad (11)$$

which involve integrals of the Langevin force. The last equality in equation (11) is obtained by integration by parts. The definition equation (11) can be generalized to an arbitrary number of integrations, with the superscript in square brackets denoting that number. Some useful properties of the W functions are derived in appendix A. Analysing equations (8) and (9) in the limit of small time step Δt we can immediately identify the stochastic lowest order terms, which are given by W, $W^{[1]}$ for the velocity and coordinate, respectively. Also, since the deterministic part of the solution does not depend on the stochastic terms, it can be found using any appropriate numerical algorithm (implicit or explicit). In addition, as we saw above, the stochastic increments $\Delta\vec{x}^{\,S}$ and $\Delta\vec{v}^{\,S}$ depend on the deterministic solution $\Delta\vec{x}^{\,D}$ implicitly through the derivatives of the drag force. It is also worth mentioning that because

the drag force $\vec{V}(\vec{x}(t))$ depends on the fluctuating coordinates of the particle, the problem equations (1) and (2) are different from standard coloured noise problems studied in [1–3].

We split each iteration in our algorithm into two steps. First, we solve the deterministic equations, i.e. equations (1) and (2) without the Langevin force, taking the full stochastic solution found at a previous moment of time $v_i(t_n)$, $x_i(t_n)$ as initial conditions. In result, we obtain the deterministic component of the solution:

$$v_i^D(t_{n+1}) = v_i(t_n) + \Delta v_i^D(\Delta t), \qquad x_i^D(t_{n+1}) = x_i(t_n) + \Delta x_i^D(\Delta t). \tag{12}$$

After that we substitute $v_i^D(t_{n+1})$, $x_i^D(t_{n+1})$ into the derivatives of the drag force in equations (8) and (9), and find $\Delta v_i^S(\Delta t)$ and $\Delta x_i^S(\Delta t)$. The latter are then used to construct a full stochastic solution at time t_{n+1}:

$$v_i(t_{n+1}) = v_i^D(t_n) + \Delta v_i^S(\Delta t), \qquad x_i(t_{n+1}) = x_i^D(t_n) + \Delta x_i^S(\Delta t). \tag{13}$$

In some sense, this approach can be regarded as a semi-implicit stochastic method, because the stochastic component of the solution at time step t_{n+1} depends on the deterministic component at the same time step. We found that such an algorithm usually provides better convergence than a fully explicit method based on substituting into $V^{(\alpha,\beta,\ldots)}$ the full solution found at t_n, i.e. $v_i(t_n)$, $x_i(t_n)$.

It is not difficult to verify that in the deterministic limit, equations (1) and (2) can become stiff when the rate of change of the drag force V is very small compared with the relaxation constant γ. To be more specific, in the one-dimensional case, the first Lyapunov exponent, which is approximately equal to γ, may significantly differ from the other exponents if $\partial_x V/\gamma \ll 1$. In addition, because the noise strength depends on γ, the stochastic part of the problem can also result in a stiff equation [5]. Since the Langevin force $\vec{\Gamma}$ behaves as $\sqrt{\gamma}$, the range of values of γ for which the stochastic and deterministic problems become stiff will be slightly different. In what follows, however, we will ignore this difference. We start by examining the non-stiff limit.

2.1. Non-stiff limit

If the relaxation time $\tau_{\mathrm{rel}} = 1/\gamma$ is not too small compared to the characteristic time scale determined by $(\partial_x V)^{-1}$, we can choose the time step Δt such that $\gamma\Delta t \ll 1$. This allows us to apply a standard explicit method for constructing the deterministic component Δx_i^D of the solution. Here, we use a fourth-order adaptive Runge–Kutta algorithm. The stochastic increments $\Delta x_i^S(\Delta t)$ and $\Delta v_i^S(\Delta t)$ are then obtained by solving equations (8) and (9) iteratively. The order of the functions W_i and $W_i^{[1]}$ appearing in these equations can be found by analysing the correlation function equation (A.5). In the limit $\gamma\Delta t \ll 1$, we find $W_i \sim O(\Delta t^{1/2})$ and $W_i^{[1]} \sim O(\Delta t^{3/2})$. More generally, it follows from equation (A.2) that $W^{[n]} \sim O(\Delta t^{n+1/2})$ and $\partial_\gamma^k W^{[n]} \sim O(\Delta t^{n+k+1/2})$. In equation (9), all derivatives of the drag force are taken at point $x_i^D(t_n + t'')$, where t'' is the integration variable. Expanding these derivatives in the vicinity of the point t_{n+1}, we obtain

$$V_i^{(\alpha)}(\vec{x}^D(t_n + t'')) \simeq V_i^{(\alpha)} - V_i^{(\alpha,\beta)} v_\beta^D(t_{n+1}) \frac{\mathrm{e}^{\gamma(\Delta t - t'')} - 1}{\gamma}, \tag{14}$$

where we have used the fact that $x_i^D(t_{n+1} - \tau) \simeq x_i^D(t_{n+1}) - \frac{1}{\gamma} v_i^D(t_{n+1})(\mathrm{e}^{\gamma\tau} - 1)$, with $\tau = \Delta t - t''$. In what follows, if not specified otherwise, all derivatives of the drag force are taken at point $x_i^D(t_{n+1})$. We note that the right-hand side of equation (14) depends only on

the deterministic solution at the moment of time t_{n+1}. To fourth order in Δt, the solution to equation (9) then reads

$$\Delta x_i^S(\Delta t) = W_i^{[1]} - V_i^{(\alpha)}\gamma \int_0^{\Delta t} \mathrm{d}t' \int_0^{t'} \mathrm{e}^{-\gamma(t'-t'')} W_\alpha^{[1]}(t'', \gamma)\, \mathrm{d}t''. \tag{15}$$

Integrating the last term in that equation using the relation equation (A.3), we finally get

$$\Delta x_i^S(\Delta t) = W_i^{[1]} - V_i^{(\alpha)}\gamma\, \partial_\gamma W_\alpha^{[2]}. \tag{16}$$

The corresponding expression for $\Delta v_i^S(\Delta t)$ is obtained by substituting equations (14) and (16) into the expansion for the velocity equation (8). Keeping terms up to the fourth order we find

$$\Delta v_i^S(\Delta t) = W_i - V_i^{(\alpha)}\gamma\, \partial_\gamma W_\alpha^{[1]} - V_i^{(\alpha,\beta)} v_\beta^D(t_{n+1}) \int_0^{\Delta t} \mathrm{e}^{-\gamma(\Delta t - t')}(\mathrm{e}^{\gamma(\Delta t - t'')} - 1) W_\alpha^{[1]}(t', \gamma)\, \mathrm{d}t'$$
$$+ \frac{\gamma}{2} V_i^{(\alpha,\beta)} G_{\alpha,\beta}^{[1]}(\Delta t, \gamma), \tag{17}$$

where we have introduced the matrix

$$G_{\alpha,\beta}^{[1]}(\Delta t, \gamma) = \int_0^{\Delta t} W_\alpha^{[1]}(t', \gamma) W_\beta^{[1]}(t', \gamma)\, \mathrm{d}t' \tag{18}$$

corresponding to a non-Gaussian stochastic term of order $O(\Delta t^4)$. Since the diagonal elements of $\hat{G}^{[1]}$ have a non-zero average, so has the stochastic correction to the velocity at the fourth order. The third term on the right-hand side of equation (17) can be integrated using equation (A.3). The stochastic correction to the velocity solution then takes the form:

$$\Delta v_i^S(\Delta t) = W_i - V_i^{(\alpha)}\gamma\, \partial_\gamma W_\alpha^{[1]} + \gamma V_i^{(\alpha,\beta)} \left[v_\beta^D(t_{n+1}) \partial_\gamma W_\alpha^{[2]} + \tfrac{1}{2} G_{\alpha,\beta}^{[1]} \right] \tag{19}$$

where we have used the relation $\overrightarrow{W}^{[2]} + \partial_\gamma \overrightarrow{W}^{[1]} = -\gamma\, \partial_\gamma \overrightarrow{W}^{[2]}$.

Equations (16) and (19) have the advantage of being easily implemented for problems in multiple dimensions. As we demonstrate in the appendix, from a numerical point of view, for each dimension, only four independent Gaussian variables are required to construct the correlated Gaussian variables as well as a Gaussian approximation for the matrix $\hat{G}^{[1]}$. Such a Gaussian approximation is the only contribution in the fourth order.

2.2. *Stiff limit*

When γ becomes very large compared to the rate of change of the drag force, the problem is found to be stiff. Choosing a time step Δt such that $\gamma \Delta t \ll 1$, as required by the algorithm developed in the previous section, can become prohibitively expensive numerically. On the other hand, choosing a larger time step in order to reduce computational time can lead to large errors in the solution. One of the main sources for such errors lies in the slow convergence of the expansions constructed above, such as the Taylor series for the different exponents. For example, an error of 10% or more is made by truncating the Taylor series of $\mathrm{e}^{-\gamma \Delta t}$ at the fourth order term if $\gamma \Delta t > 1.3$. We also note that the stochastic terms in the solution behave differently in the limit of large γ, because the noise strength q increases with γ. Using the correlation functions equation (A.5) we find, in that limit, $W_i \sim O(\Delta t^0)$ and $W_i^{[1]} \sim O(\Delta t^{1/2})$. This leads to the classical result for Brownian motion in the absence of an external potential, i.e. $\langle \vec{v}^2 \rangle = \frac{3}{2} kT/m$ and $\langle \vec{x}^2 \rangle = 6Dt$, where D is the diffusion constant.

In order to rigorously investigate the stiff limit, we formally assume that $\tau_{\mathrm{rel}} \sim O(\epsilon^2)$, $\Delta t \sim O(\epsilon)$ and study equations (1) and (2) with respect to the new small parameter ϵ. Were the order of τ_{rel} even higher, the accuracy of the estimates provided below would only improve. We start by identifying the order of the different random Gaussian variables in

the problem. Using equations (A.4), it is easy to show that $W(\Delta,\gamma)\sim O(\epsilon^0)$, $W(\Delta,0)\sim O(\epsilon^{-1/2})$, and each derivative of $W(\Delta,\gamma)$ with respect to γ taken at the point $\gamma=0$ increases its order in ϵ by 1. Here, we took into account that $q\sim\epsilon^{-2}$. Hence, the lowest order term in equation (A.2) is proportional to $\frac{1}{\gamma}(\partial_\gamma)^{n-1}W(\Delta t,\gamma)|_{\gamma=0}\sim O(\epsilon^{n+1/2})$ and therefore $W^{[n]}\sim O(\epsilon^{n+1/2})$.

We then note that since $\gamma\Delta t\sim O(1/\epsilon)$, the exponent $\mathrm{e}^{-\gamma\Delta t}$ is of higher order than any power of ϵ. As a result, we can neglect all terms proportional to that exponent in the final expressions. Furthermore, in the leading order of ϵ, the kernel $\gamma\mathrm{e}^{-\gamma(t'-t'')}$ in the integral equations (8) and (9) can be replaced by $\delta(t'-t'')$. It is not difficult to verify that in order to construct a stochastic solution valid to fourth order in ϵ, we need an expression for $\Delta\vec{x}^{\,D}$ which is valid to second order only. Such an expression can be obtained by first rewriting equation (2) as

$$v_i^D(t_{n+1}-\tau)=V_i\big(x_i^D(t_{n+1}-\tau)\big)+\frac{1}{\gamma}\frac{\mathrm{d}}{\mathrm{d}\tau}v^D{}_i(t_{n+1}-\tau).$$

Iterating the latter we obtain for the coordinate, in the second order:

$$x_i^D(t_{n+1}-\tau)\simeq x_i^D(t_{n+1})-V_i\tau-\frac{1}{\gamma}\big[V_i-v_i^D(t_{n+1})\big]+V_i^{(\alpha)}V_\alpha\frac{\tau^2}{2}. \tag{20}$$

Note that the last two terms in equation (20) are of the same order with respect to ϵ. Following the procedure described in the previous section and expanding the derivatives of the drag force in equation (9), we obtain, in the fourth order,

$$\Delta x_i^S(\Delta t)=W_i^{[1]}-V_i^{(\alpha)}\gamma\partial_\gamma W_\alpha^{[2]}+V_i^{(\alpha,\beta)}V_\alpha\gamma\partial_\gamma W_\beta^{[3]}+V_i^{(\alpha)}V_\alpha^{(\beta)}\frac{\gamma^2}{2}\partial_\gamma^2W_\beta^{[3]}+\frac{1}{2}V_i^{(\alpha,\beta)}G_{\alpha,\beta}^{[1]}. \tag{21}$$

Note that in the limit of small relaxation time, the fourth-order stochastic correction to the coordinate solution has a nonzero average due to the presence of the matrix $\hat{G}^{[1]}$. The term causing such a drift is proportional to the second derivative of the drag force. We can estimate the leading order in the drift term:

$$\big\langle G_{\alpha,\alpha}^{[1]}(\Delta t,\gamma)\big\rangle\simeq\frac{q\Delta t^2}{2\gamma^2}.$$

It is indeed of the fourth order with respect to ϵ.

Following the same line of analysis we can calculate the stochastic part of the velocity solution. Expanding the derivatives of the drag force and keeping only important terms we find

$$\begin{aligned}\Delta v_i^S(\Delta t)=W_i&+\gamma V_i^{(\alpha)}\int_0^{\Delta t}\mathrm{e}^{-\gamma(\Delta t-t')}\Delta x_\alpha^S(t')\,\mathrm{d}t'\\&-\gamma V_i^{(\alpha,\beta)}\int_0^{\Delta t}\mathrm{e}^{-\gamma(\Delta t-t')}\left[(\Delta t-t')V_\alpha+\frac{V_\alpha-v_\alpha^D}{\gamma}\right]\Delta x_\beta^S(t')\,\mathrm{d}t'\\&+\frac{1}{2}V_i^{(\alpha,\beta)}\int_0^{\Delta t}\mathrm{e}^{-\gamma(\Delta t-t')}\Delta x_\alpha^S(t')\Delta x_\beta^S(t')\,\mathrm{d}t'.\end{aligned} \tag{22}$$

We can neglect the last term in equation (20), which is proportional to $(\Delta t-t')^2$, because it disappears after the integration due to $\gamma\mathrm{e}^{-\gamma(\Delta t-t')}\sim\delta(\Delta t-t')$. Substituting equation (21) into (22) we obtain the stochastic correction:

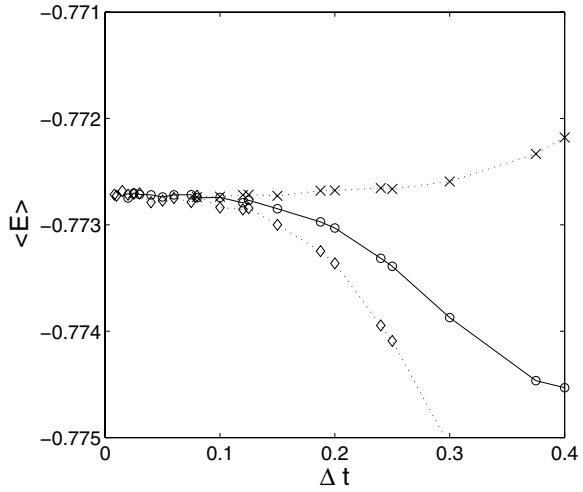

Figure 1. The convergence of various fourth-order algorithms for solving the Duffing model. The average energy $\langle E\rangle$ is calculated at a finite time $t = 6$ ($\frac{m}{kT} = 5$ and $\gamma = 1$). Initial position and velocity were set to zero in this and following calculations. The average energy is calculated on a sample of 2×10^8 trajectories. Diamonds: Hershkowitz's algorithm [7]. Circles: the algorithm described in section 2. Crosses: Drozdov and Brey's algorithm described in equations (38)–(42) of paper [9].

$$\Delta v_i^S(\Delta t) = W_i - \gamma\left[\left(V_i^{(\alpha)} - V_i^{(\alpha,\beta)}\frac{V_\beta - v_\beta^D}{\gamma}\right)\partial_\gamma + \frac{1}{2}V_i^{(\alpha,\beta)}V_\beta\partial_\gamma^2\right]W_\alpha^{[1]} + V_i^{(\alpha)}V_\alpha^{(\beta)}\frac{\gamma^2}{2}\partial_\gamma^2 W_\beta^{[2]}$$
$$- V_i^{(\alpha)}\left[V_\alpha^{(\beta,\kappa)}V_\beta\frac{\gamma^2}{2}\partial_\gamma^2 + V_\alpha^{(\beta)}V_\beta^{(\kappa)}\frac{\gamma^3}{6}\partial_\gamma^3\right]W_\kappa^{[3]} + \mathrm{NG}_i. \tag{23}$$

The last term describes a non-Gaussian contribution to the solution and it reads

$$\mathrm{NG}_i = \frac{1}{2}V_i^{(\alpha)}V_\alpha^{(\beta,\kappa)}G_{\beta,\kappa}^{[1]} + \gamma^2 V_i^{(\alpha,\beta)}V_\alpha^{(\kappa)}\partial_\gamma W_\beta^{[1]}\partial_\gamma W_\kappa^{[2]}$$
$$- \frac{\gamma}{2}V_i^{(\alpha,\beta)}\left[W_\alpha^{[1]}\partial_\gamma W_\beta^{[1]} + \partial_\gamma W_\alpha\partial_\gamma W_\beta^{[1]} - \partial_\gamma W_\alpha\partial_\gamma W_\beta\right].$$

3. One-dimensional Duffing equation

In order to compare different numerical methods for solving SDEs in asymptotic or stiff regimes, a simple, one-dimensional model is often utilized. The model, called the Duffing oscillator [12], describes a nonlinear oscillator with bistable potential

$$U(x) = x^4 - 2x^2, \qquad V(x) = -\partial_x U(x) = -4(x^3 - x). \tag{24}$$

Different approaches have been proposed to tackle this problem numerically. The most straightforward method, based on an expansion in $\gamma\Delta t \ll 1$, is provided in [7]. Another numerical approach that is based on operator expansion of the evolution operator, demonstrated much better converges in the limit $\gamma\Delta t \ll 1$ [8–10]. Our semi-implicit method described in section 2.1 is compared to Hershkovitz's and Drozdov and Brey's algorithms in figure 1 which shows how the average energy of the system at time $t = 6$ (see [10]) depends on the time step for a relaxation rate $\gamma = 1$. The figure shows that the average energy converges to the correct

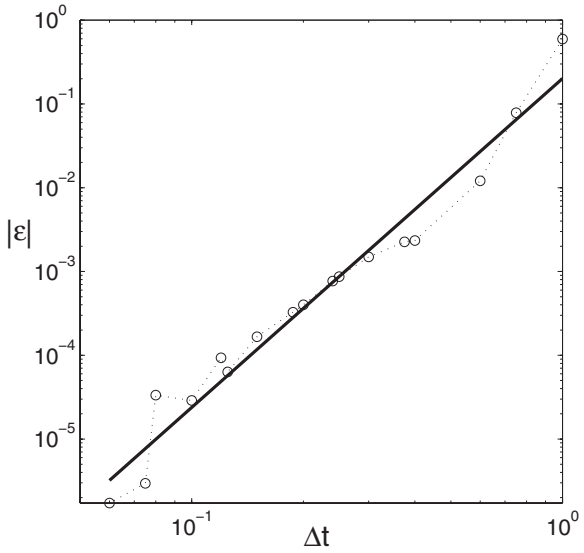

Figure 2. The relative error $\epsilon = [\langle E\rangle - E_0]/E_0$ as a function of time step. Circles: average energy calculated using the algorithm described in section 2. The fitted line has slope $n = 3.9$.

value $E_0 = -0.77272$ faster with the algorithm developed in section 2.1 (circles, in the figure) than with the method of paper [7]. The best performance in terms of convergence is obtained with the algorithm due to Drozdov and Brey. The order of convergence of our algorithm is demonstrated on the log–log plot shown in figure 2. A linear fit gives a slope equal to 3.9, confirming the fourth-order dependence of the error on the time step.

The advantage of our approach is readily observed in the overdamped regime. In the regime of large γ, the algorithm of section 2.2 provides significantly better convergence than other methods, thus allowing a large increase in the algorithm's time step (see figure 3). As can be seen from figure 3, the performance of Drozdov and Brey's algorithm deteriorates with increasing γ and the error ϵ grows exponentially as $\gamma\Delta t$ becomes larger than 1 (dotted lines in the figure). By contrast, the algorithm developed in section 3 exhibits much more stability with respect to the magnitude of the time step (solid lines). It is also important to note that, at fixed time step Δt and with increasing γ, the latter only improves in convergence whereas the other algorithms diverge even faster.

4. Motion of airborne particles through random fibre networks

We now turn to the problem of predicting the filtration efficiency of random fibre networks. The model filters consist of fibres of diameters 1 and 4 μm mixed together in different proportions. These fibre diameters were chosen in order to facilitate comparisons with the experimental work of Browne and Thorpe [18], who evaluated filters made from glass fibres of similar dimensions. Our simulated filters were created using a model originally proposed to predict the structure of paper and how it deforms under compressive forces [19]. Five different structures were created, corresponding to five different values for the weight fraction of the large fibres f_4 (0.1, 0.3, 0.5, 0.7 and 0.9). The filter generated in the case $f_4 = 0.7$ is shown in the inset of figure 4. That particular network consists of 24 fibres of diameter $d_f = 4\,\mu$m and 192 fibres of diameter $d_f = 1\ \mu$m contained in a simulation domain of size $40 \times 40\,\mu\text{m}^2$,

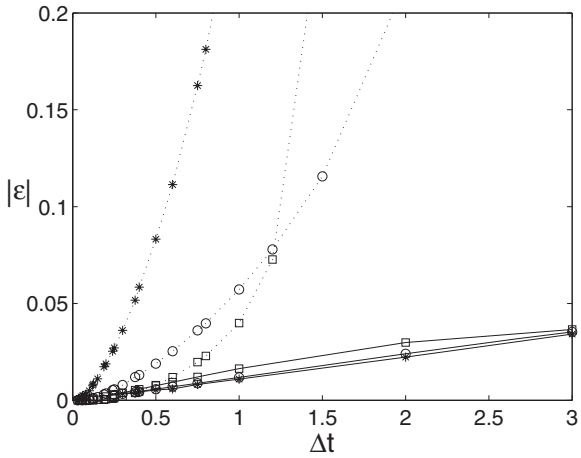

Figure 3. The relative error $\epsilon = [\langle E\rangle - E_0]/E_0$ of Duffing oscillator solution in the overdamped limit. The average energy $\langle E\rangle$ is calculated at a finite time of $t = 12$ with $\frac{m}{kT} = 5$ and initial position and velocity set to zero. The value E_0 is taken as $\langle E\rangle$ calculated at $\Delta t = 0.03$. The algorithm of section 2 corresponds to solid lines and the algorithm of Drozdov and Brey is represented by dotted lines. Squares: $\gamma = 25$, circles: $\gamma = 50$, asterisks: $\gamma = 100$.

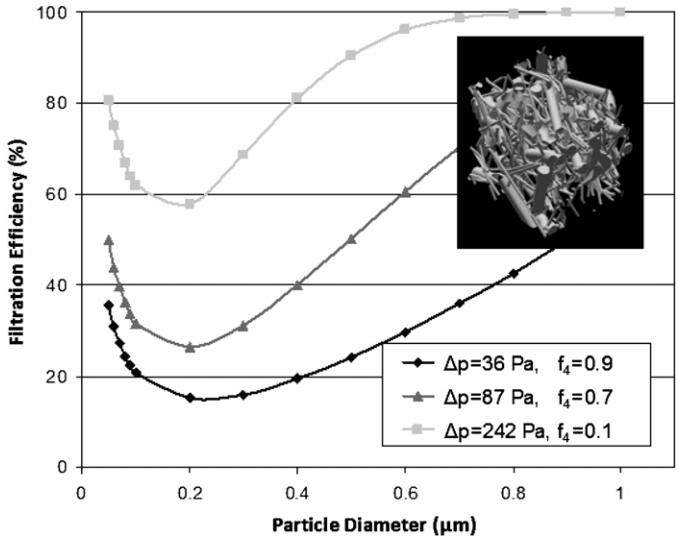

Figure 4. Filtration efficiency of three different filters with bimodal fibre size distribution. The face velocity was set to 10 $\mathrm{cm\,s^{-1}}$ in all cases. The inset shows the simulated filter structure corresponding to a long fibre weight fraction $f_4 = 0.7$.

discretized at a resolution $\mathrm{d}x = 62.5$ nm. The porosity of that structure as well as that of all others in the study was set to 85%.

Before computing trajectories of airborne particles moving through our model structures, the flow field $V(\vec{x})$ appearing in equation (2) must be calculated. Here that step was performed using a Lattice–Boltzmann method [20]. As an example, discretization of the fibre network shown in figure 4 required $794 \times 640 \times 640$ nodes. The pressure drop ΔP applied across

the thickness of the filter was adjusted so that the velocity of air as it approaches the filter is $10\,\mathrm{cm\,s^{-1}}$.

Having the three-dimensional velocity profile $\vec{V}(\vec{x})$, we can now construct particle trajectories using equation (2). The particles are initially distributed along a plane located upstream from the filter and perpendicular to the flow. We assume that the initial velocity of the particles coincides with the air flow velocity, i.e. $\vec{v}_0 = \vec{V}(\vec{x}_0)$. In the calculation, the deterministic component of the solution is obtained using either an adaptive fourth-order Runge–Kutta algorithm when γ is small (large particle) or an implicit algorithm also with adaptive step size control in the case of large γ (small particle). In addition to being more efficient, the implicit algorithm avoids accumulating large errors in interpolating $\vec{V}(\vec{x})$ between neighbouring nodes on the lattice. If the time step of the algorithm becomes too small, the accumulated interpolation error can exceed that from the algorithm itself. The stochastic components of the solution are obtained using equations (16), (19) and (21), (23), respectively. The calculation proceeds until the particle is either captured or exits from the other side of the filter. A particle is assumed to be captured when the distance between its centre of mass and the closest fibre in the network becomes less than the particle's radius. The filtration efficiency at a given particle size is obtained by repeating the calculation for a large number of particles starting from different initial positions.

Figure 4 shows the efficiency curves obtained for three of our structures and for airborne particle sizes varying between 50 nm and 1 μ m in size. All three curves exhibit a minimum at an airborne particle size around 200 nm which is typical of fibrous filters. In the region to the left of this minimum, capture occurs mostly through Brownian diffusion while to the right, the dominant mechanisms are interception and, for larger particles, inertial impaction. The filtration efficiency increases as the fraction of large fibres in the mixture decreases and so does the pressure drop required to achieve a flow velocity of $10\,\mathrm{cm\,s^{-1}}$. Our results also show that the minimum in the curve moves to the left and becomes sharper as f_4 decreases. All of these trends agree with the experimental observations of Browne and Thorpe who obtained similar curves for filter samples made from a binary mixture of glass fibres. A more detailed account of our study as well as of its implications for filter design optimization will be presented elsewhere.

5. Concluding remarks

We have proposed two fourth-order numerical algorithms for solving SDEs in different regimes. These algorithms have a very general form and can be applied to solving multi-variable problems without any further modification of the algorithms themselves. We have demonstrated that in the standard non-stiff limit, the semi-implicit algorithm of section 2 has a convergence rate comparable to that of other existing methods [9]. In the stiff limit where standard approaches do not work well, the algorithm of section 3 exhibits excellent convergence with respect to the time step Δt. The method is very stable in the region of parameters where other available approaches usually fail.

Both stiff and non-stiff algorithms are called semi-implicit, because the stochastic component of the solution at the time step t_{n+1} formally depends on the deterministic component at the same time step. The deterministic component can be calculated using any numerical method considered appropriate for a particular problem. The stochastic part of the solution requires evaluation of up to third-order partial derivatives of the potential, as many other fourth-order algorithms for solving Langevin equations of this type would. Therefore, for multi-dimensional problems, solving the corresponding Fokker–Planck equation could be more convenient in some cases.

The stochastic method that we developed is based on W-functions and does not depend on a particular form of the noise. Therefore, it can also be applied to problems with Ornstein–Uhlenbeck or other types of non-white noise. One would only need to recalculate the correlation coefficient $C_{i,j}(\omega, \omega')$ defined in equation (A.4).

Acknowledgments

The authors gratefully acknowledge the financial support of the NSERC-Sentinel Bioactive Paper Network. We would also like to thank Jorge Viñals for several insightful discussions and David Vidal and François Bertrand for providing us with the Lattice–Boltzmann code used to calculate the flow field in section 4.

Appendix A. Algebra of W functions

In equations (10) and (11) we defined two Gaussian variables. We can generalize the definition to the case of multiple integrals:

$$\overrightarrow{W}^{[n]}(\Delta t, \omega) = \int_0^{\Delta t} \vec{W}^{[n-1]}(\tau', \omega)\, \mathrm{d}\tau' = -\frac{\overrightarrow{W}^{[n-1]}(\Delta t, \omega) - \overrightarrow{W}^{[n-1]}(\Delta t, 0)}{\omega}. \tag{A.1}$$

It is not difficult to show that

$$\overrightarrow{W}^{[n]}(\Delta t, \omega) = \frac{1}{(-\omega)^n}\left[\overrightarrow{W}(\Delta t, \omega) - \sum_{k=0}^{n-1} \frac{\omega^k}{k!}\partial_\omega^k \overrightarrow{W}(\Delta t, \omega)|_{\omega=0}\right], \tag{A.2}$$

We can also generalize the relation equation (11) as follows:

$$\int_0^{\Delta t} \mathrm{e}^{-\omega'(\Delta t - t')}\overrightarrow{W}^{[n]}(t', \omega)\, \mathrm{d}t' = -\frac{\overrightarrow{W}^{[n]}(\Delta t, \omega) - \overrightarrow{W}^{[n]}(\Delta t, \omega')}{(\omega - \omega')}. \tag{A.3}$$

Indeed, for $\overrightarrow{W}$ function equation (A.3) can be verified directly. The higher order relations are proved based on equation (A.1) and using the recurrent method. If $\omega' = \omega$ we obtain a simple integro-differential relation, which greatly simplifies integral expressions in the stochastic solution.

We note that all $\vec{W}^{[n]}$ are correlated. The correlation function of $\overrightarrow{W}$ reads

$$C_{i,j}(\omega, \omega') \equiv \langle W_i(\Delta t, \omega) W_j(\Delta t, \omega')\rangle = \frac{q}{\omega + \omega'}(1 - \mathrm{e}^{-(\omega+\omega')\Delta t})\, \delta_{ij}. \tag{A.4}$$

Using the relation equation (A.2) and performing simple algebra one can easily confirm [2]

$$\begin{aligned}
\langle W_i(\Delta t, \gamma) W_j(\Delta t, \gamma)\rangle &= \frac{q}{2\gamma}(1 - \mathrm{e}^{-2\gamma\Delta t})\delta_{ij},\\
\left\langle W_i(\Delta t, \gamma) W_j^{[1]}(\Delta t, \gamma)\right\rangle &= \frac{q}{2\gamma^2}(1 - \mathrm{e}^{-\gamma\Delta t})^2\delta_{ij},\\
\left\langle W_i^{[1]}(\Delta t, \gamma) W_j^{[1]}(\Delta t, \gamma)\right\rangle &= \frac{q}{2\gamma^3}(2\gamma\Delta t - 3 - \mathrm{e}^{-2\gamma\Delta t} + 4\,\mathrm{e}^{-\gamma\Delta t})\, \delta_{ij}.
\end{aligned} \tag{A.5}$$

Using the correlation function equation (A.4) and the expansion equation (A.1), it is not difficult to find higher order correlation functions $\left\langle W_i^{[n]}(\Delta t, \omega) W_j^{[k]}(\Delta t, \omega')\right\rangle$, because the differentiation with respect to ω commutes with the averaging procedure.

Appendix B. Gaussian representation of W functions

As we demonstrated in this paper, in order to construct a stochastic solution of equations (1) and (2) we need from four to six Gaussian variables for each dimension depending on the type of the problem. In the non-stiff case, those are W_i, $W_i^{[1]}$, $\partial_\gamma W_i^{[1]}$, $\partial_\gamma W_i^{[2]}$. For calculating correlation functions of different variables it is more convenient to choose a different basis W_i, $W_i^{[1]}$, $\partial_\gamma W_i$, $W_i^{[2]}$. As we demonstrate below, in the stiff case we need to add only two more variables $W_i^{[3]}$, $\partial_\gamma^2 W_i$. The derivatives of higher order W functions that are involved in the computation of the solution equations (16) and (19) can be constructed from a simple relation (see equation (A.1)):

$$\gamma\partial_\gamma W_i^{[n]} = -W_i^{[n]} - \partial_\gamma W_i^{[n-1]}. \tag{B.1}$$

Hence, we obtain

$$\gamma\partial_\gamma W_i^{[1]} = -W_i^{[1]} - \partial_\gamma W_i, \qquad \gamma\partial_\gamma W_i^{[2]} = -W_i^{[2]} + \frac{1}{\gamma}W_i^{[1]} + \frac{1}{\gamma}\partial_\gamma W_i. \tag{B.2}$$

For the stiff problem solution equations (21) and (23) we are interested in the terms up to ϵ^4 and therefore, some expressions greatly simplify:

$$\frac{\gamma^2}{2}\partial_\gamma^2 W_i^{[1]} = W_i^{[1]} + \partial_\gamma W_i - \frac{\gamma}{2}\partial_\gamma^2 W_i, \qquad \frac{\gamma^2}{2}\partial_\gamma^2 W_i^{[2]} = W_i^{[2]} - \frac{2}{\gamma}W_i^{[1]} + \frac{1}{2}\partial_\gamma^2 W_i,$$

$$\gamma\partial_\gamma W_i^{[3]} = -W_i^{[3]} + O\big(\epsilon^{4\frac{1}{2}}\big), \qquad \frac{\gamma^2}{2}\partial_\gamma^2 W_i^{[3]} = W_i^{[3]} + O\big(\epsilon^{4\frac{1}{2}}\big),$$

$$\frac{\gamma^3}{6}\partial_\gamma^2 W_i^{[3]} = -W_i^{[3]} + O\big(\epsilon^{4\frac{1}{2}}\big).$$

Hence, the more complex implicit solution can be simplified and written in a compact form:

$$\Delta x_i^S(\Delta t) = W_i^{[1]} - V_i^{(\alpha)}\gamma\partial_\gamma W_\alpha^{[2]} + \big(V_i^{(\alpha)}V_\alpha^{(\beta)} - V_i^{(\alpha,\beta)}V_\alpha\big)W_\beta^{[3]} + \frac{1}{2}V_i^{(\alpha,\beta)}G_{\alpha,\beta}^{[1]},$$

$$\Delta v_i^S(\Delta t) = W_i - \gamma\left[\left(V_i^{(\alpha)} - V_i^{(\alpha,\beta)}\frac{V_\beta - v_\beta^D}{\gamma}\right)\partial_\gamma + \frac{1}{2}V_i^{(\alpha,\beta)}V_\beta\partial_\gamma^2\right]W_\alpha^{[1]}$$
$$+ V_i^{(\alpha)}V_\alpha^{(\beta)}\frac{\gamma^2}{2}\partial_\gamma^2 W_\beta^{[2]} + V_i^{(\alpha)}\big[V_\alpha^{(\beta)}V_\beta^{(\kappa)} - V_\alpha^{(\beta,\kappa)}V_\beta\big]W_\kappa^{[3]} + \mathrm{NG}_i.$$

Below we reduce the notations to a one-dimensional case and drop the index of dimension in W functions. A generalization to an arbitrary number of dimensions is straightforward. We will start from the non-stiff limit. Four basis Gaussian variables W, $W^{[1]}$, $\partial_\gamma W$, $W^{[2]}$ can be represented as linear combinations of four normally distributed variables $Y_m, m = 0,\ldots,3$ with zero average and standard deviation equal 1. Starting from the lowest order function $W = \sqrt{C(\gamma,\gamma)}Y_0$, and using equations (A.2), (A.4) we can construct the linear combinations as follows:

$$W^{[1]} = \sum_{m=0}^{1} A_m(W^{[1]})Y_m,\ A_0(W^{[1]}) = \frac{\langle W W^{[1]}\rangle}{\sqrt{C(\gamma,\gamma)}},$$

$$A_1(W^{[1]}) = \sqrt{\langle W^{[1]}W^{[1]}\rangle - A_0(W^{[1]})^2},$$

$$\partial_\gamma W = \sum_{m=0}^{2} A_m(\partial_\gamma W)Y_m,\ A_0(\partial_\gamma W) = \frac{\langle W\partial_\gamma W\rangle}{\sqrt{C(\gamma,\gamma)}},$$

$$A_1(\partial_\gamma W) = \frac{\langle W^{[1]}\partial_\gamma W\rangle - A_0(W^{[1]})A_0(\partial_\gamma W)}{A_1(W^{[1]})},$$

$$A_2(\partial_\gamma W) = \sqrt{\langle \partial_\gamma W \partial_\gamma W\rangle - A_0(\partial_\gamma W)^2 - A_1(\partial_\gamma W)^2},$$

$$W^{[2]} = \sum_{m=0}^{3} A_m(W^{[2]})Y_m,\ A_0(W^{[2]}) = \frac{\langle W W^{[2]}\rangle}{\sqrt{C(\gamma,\gamma)}},\ldots. \tag{B.3}$$

We note that the calculation of the coefficients A_m is very straightforward, because all correlation functions can be calculated using $C(\omega,\omega')$ or its derivatives with respect to one of the arguments.

It follows from the definition equation (18) that the non-Gaussian variable $G^{[1]}$ is of order Δt^4 in the non-stiff limit or ϵ^4 in the stiff limit. Therefore, any non-Gaussian corrections to a Gaussian approximation can be ignored due to their higher order. In the non-stiff limit, the four variables Y_m are sufficient. Indeed, in the leading order two variables $W^{[1]}$ and $\partial_\gamma W$ are identical (see equation (B.2)). We can also ignore the correlation function with $\langle(\partial_\gamma^2 W)^2\rangle$ and $\langle(W^{[2]})^2\rangle$, because they are of order Δt^5. So, the non-Gaussian variable approximately reads

$$G^{[1]} = \frac{q\Delta t^4}{2}\left[\bar{P} + P_0 Y_0^2 + P_{01}Y_0Y_1 + P_1Y_1^2 + P_{02}Y_0Y_2 + P_{12}Y_1Y_2 + P_2Y_2^2\right]. \tag{B.4}$$

Here,

$$\bar{P} = \frac{1}{210} - \frac{1}{140}\sqrt{\frac{33}{2}}, \qquad P_0 = \frac{1}{10}, \qquad P_{01} = \frac{4}{15\sqrt{3}}, \qquad P_1 = \frac{13}{210},$$

$$P_{02} = \frac{1}{21\sqrt{5}}, \qquad P_{12} = \frac{1}{12\sqrt{15}}, \qquad P_2 = \frac{1}{140}\sqrt{\frac{33}{2}}.$$

The first term is responsible for the nonzero average of $G^{[1]}$ itself and each $\langle Y_m^2\rangle = 1$, whereas the last term insures a correct second moment $\langle(G^{[1]})^2\rangle$. In the stiff limit we add two more basis elements $W_i^{[3]}$, $\partial_\gamma^2 W_i$, which are constructed using two additional normalized variables Y_4, Y_5 following the form of equation (B.3). In terms of ϵ the order of the basis variables $\left(W, W^{[1]}, \partial_\gamma W, W^{[2]}, W_i^{[3]}, \partial_\gamma^2 W_i\right)$ is $\left(0, \frac{3}{2}, 2, \frac{5}{2}, \frac{7}{2}, 4\right)$, accordingly. The form of the non-Gaussian variable is again simplified if we neglect terms of order higher than ϵ^4. It reads

$$G^{[1]} = \frac{q\Delta t^2}{2\gamma^2}\left[\bar{P} + P_0 Y_0^2 + P_{01}Y_0Y_1 + P_1Y_1^2 + P_{02}Y_0Y_2 + P_{12}Y_1Y_2 \right.$$
$$\left. + P_2Y_2^2 + P_{03}Y_0Y_3 + P_{13}Y_1Y_3 + P_{04}Y_0Y_4 + P_{05}Y_0Y_5 + P_3Y_3^2\right]. \tag{B.5}$$

The last term insures a correct value of the second moment. Values of the constants P are different from those of the non-stiff case and can be easily calculated.

References

[1] Sancho J M, SanMiguel M, Katz S L and Gunton J D 1982 *Phys. Rev.* A **26** 1589
[2] Mannella R and Palleschi V 1989 *Phys. Rev.* A **40** 3381
[3] Fox R F 1991 *Phys. Rev.* A **43** 2649
[4] Drummond P D and Mortimer I K 1991 *J. Comput. Phys.* **93** 144
[5] Kloeden P E and Platen E 1992 *J. Stat. Phys.* **66** 283
[6] Honeycutt R L 1992 *Phys. Rev.* A **45** 600
[7] Hershkovitz E 1998 *J. Chem. Phys.* **108** 9253
[8] Drozdov A N and Brey J J 1998 *Phys. Rev.* E **57** 1284
[9] Forbert H A and Chin S A 2000 *Phys. Rev.* E **63** 016703

[10] Bao J-D, Li R-W and Wu W 2004 *J. Comput. Phys.* **197** 241
[11] Finlay W 2001 *The Mechanics of Inhaled Pharmaceutical Aerosols* (London: Academic)
[12] Bixon M and Zwanzig R 1971 *J. Stat. Phys.* **3** 245
[13] Newman T J, Bray A J and McKane A J 1990 *J. Stat. Phys.* **59** 357
[14] Rahman M 1996 *Phys. Rev.* E **53** 6547
[15] Mallick K and Marcq P 2004 *Eur. Phys. J.* B **38** 99
[16] Fox R F 1998 *Phys. Rev.* E **57** 2177
[17] Fox R F and Choi M H 2001 *Phys. Rev.* E **63** 051901
[18] Browne R C and Thorpe A 2001 *Powder Technol.* **118** 3
[19] Drolet F and Uesaka T 2005 *Advances in Paper Science and Technology, FRC* (Lancashire: The Pulp and Paper Fundamental Research Society)
[20] Vidal D, Ridgway C, Pianet G, Schoelkopf J, Roy R and Bertrand F 2009 *Comput. Chem. Eng.* **33** 256